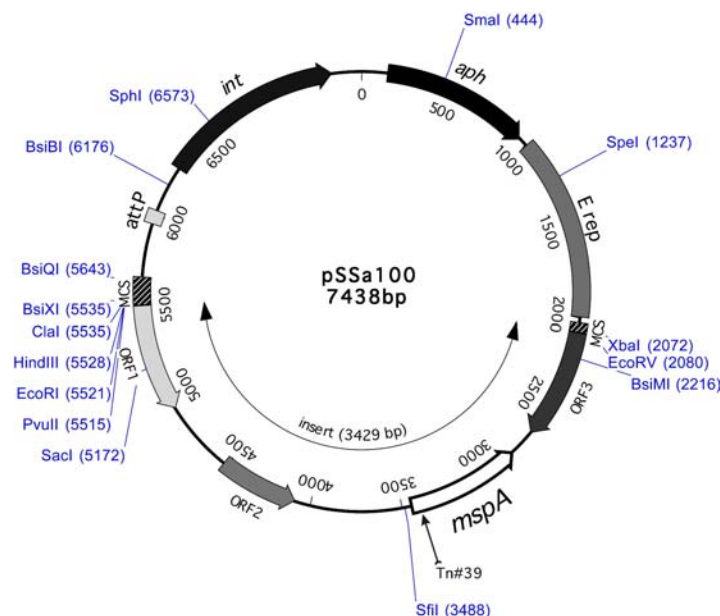


### 3 Results

#### 3.1 Heterologous expression of the porin MspA from *M. smegmatis* in *M. bovis* BCG affects its *in vitro* growth and intracellular persistence.

##### 3.1.1 Introduction of *mspA* into *M. bovis* BCG

The lack of efficient porins like MspA in the cell wall of slow-growing mycobacteria like *M. bovis* BCG motivated me to transfer a genomic region of *M. smegmatis* comprising *mspA* into *M. bovis* BCG. A 3429 bp DNA fragment containing *mspA* was obtained by PCR and was cloned in the integrative plasmid pMV306 (see section 2.7.1). The generated recombinant plasmid (pSSa100) contained besides *mspA* three other open reading frames (ORFs). Two ORFs were located upstream and one downstream of *mspA* (Figure 2). A blast search (<http://www.ncbi.nlm.nih.gov/BLAST/>) revealed ORF1 to be highly homologous to a TetR-family transcriptional regulator of *Streptomyces coelicolor*. ORF2 had a low homology to a putative oxidase of *S. coelicolor*. ORF3 located downstream of *mspA* showed a high homology to a putative protein of *M. tuberculosis* CDC1551. Sequencing of the insert of pSSa100 revealed rMspA to contain no amino acid replacements.



**Figure 2:** Map of the plasmid pSSa100. A 3429 bp fragment containing the porin gene *mspA* was obtained from genomic DNA of *M. smegmatis* by PCR and was cloned into the unique *EcoRV* site of the plasmid pMV306. The arrow indicates the location of a transposon insertion in a mutant derivative (Tn#39) of pSSa100. *aph*: aminoglycoside phosphotransferase; *attP*: attachment site of phage L5; *Erep*: origin of replication of pUC plasmids; *int*: integrase gene; MCS: multiple cloning site.

After introduction of pSSa100 into *M. bovis* BCG via electroporation I could detect a growth advantage of *M. bovis* BCG (pSSa100) in comparison with the reference *M. bovis* BCG (pMV306). Colonies of *M. bovis* BCG containing the *mspA* gene appeared about one or two days earlier than the reference (data not shown). By performing PCR with primers specific for the *aph* gene of pMV306 (conferring kanamycin resistance) and for the *mspA* gene, I could show that *mspA* and *aph* were stably integrated into the genome of the *M. bovis* BCG transformants and were not lost throughout the entire experiments (data not shown).

### 3.1.2 *MspA* is expressed in *M. bovis* BCG containing pSSa100

To investigate the expression of *mspA* in the *M. bovis* BCG derivative, I performed RT-PCRs. In addition, the expression of the selection marker *aph* of pSSa100 was chosen as a reference for expression of a gene introduced with the same vector system into *M. bovis* BCG. Total RNA was isolated from cultures of *M. bovis* BCG (pSSa100) and *M. bovis* BCG (pMV306) and RT-PCRs were performed using specific primers binding to *mspA* and *aph*. As shown in Figure 3 A, lane 2 and 3, an *mspA* specific RT-PCR product of 228 bp was only obtained by using RNA from *M. bovis* BCG (pSSa100). In addition, a 556 bp fragment specific for *aph* was amplified using RNA preparations of both strains (Figure 3 A, lanes 5 and 6). These results demonstrate the successful transcription of the recombinant *mspA* in the *M. bovis* BCG derivative.

Next it had to be answered, if translation of *mspA* mRNA in *M. bovis* BCG occurred. Therefore, Western blots with protein isolations from both *M. bovis* BCG strains and *M. smegmatis* were performed. The selective extraction of MspA from *M. smegmatis* according to the method of Heinz and Niederweis (2000) showed on a 10% SDS-polyacrylamide gel the oligomer of MspA (data not shown), which was recognized by the polyclonal rabbit antiserum (pAK MspA#813) in Western blot experiments (Figure 3 B, lane 1). However, the selective isolation of rMspA with nOPOE from *M. bovis* BCG was not as effective as the isolation of MspA from *M. smegmatis*. Therefore, the cell mass of *M. bovis* BCG used for the isolation of proteins was increased and about 350 mg of *M. bovis* BCG (wet weight) was employed. Although SDS-PAGE of these extracts did not show a defined band for rMspA even after silver staining (data not shown), a clear signal for the oligomeric form of rMspA was detected in extracts from the *M. bovis* BCG derivative with pSSa100 in Western blot experiments (Figure 3 B, lane 2). Hereby I evidenced the synthesis of oligomeric rMspA in *M. bovis* BCG

(pSSa100). However, the amount of rMspA in *M. bovis* BCG was clearly decreased if compared with *M. smegmatis*. As expected, the reference strain *M. bovis* BCG (pMV306) produced no signal with the MspA antiserum (Figure 3 B, lane 3).

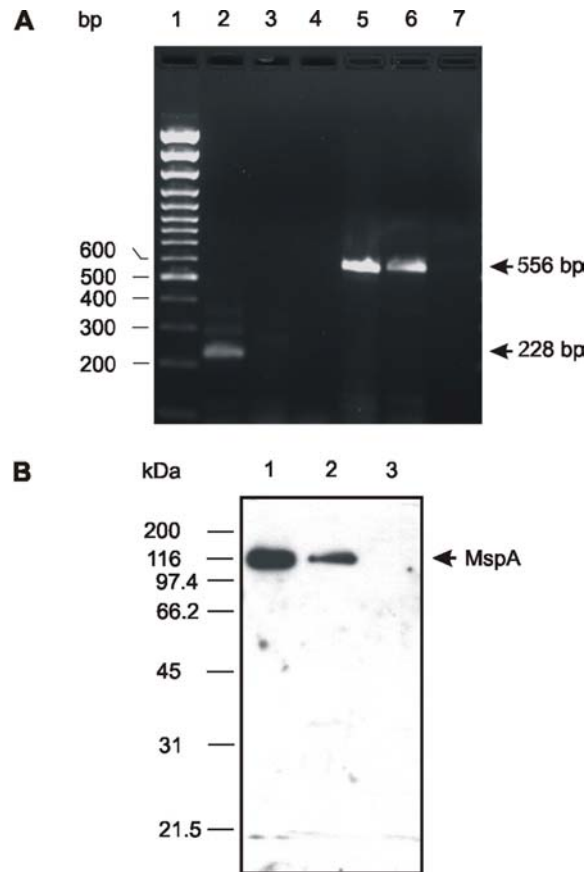


**Figure 3:** Expression analysis of *mspA* in *M. bovis* BCG derivatives by RT-PCR and Western blotting. A. Transcription analysis of *mspA* in *M. bovis* BCG derivatives by RT-PCR. The successful transcription of the recombinant porin in *M. bovis* BCG (pSSa100) is demonstrated by the band of 228 bp (see lane 2) using specific primers for *mspA*. As a control the transcription of the selection marker *aph* is demonstrated by amplifying a fragment of 556 bp (see lanes 5 and 6). Lane 1, 100 bp DNA ladder; lanes 2-4, RT-PCR with specific primers for *mspA*; lane 2, *M. bovis* BCG (pSSa100); lane 3, *M. bovis* BCG (pMV306); lane 4, no template control; lanes 5-7, RT-PCR with specific primers for *aph*; lane 5, *M. bovis* BCG (pSSa100); lane 6, *M. bovis* BCG (pMV306); lane 7, no template control. B. Western blot analysis of isolated proteins from *M. bovis* BCG derivatives and *M. smegmatis*. Proteins from *M. bovis* BCG derivatives and *M. smegmatis* were isolated using the detergent nOPOE. The samples from the *M. bovis* BCG derivatives and *M. smegmatis* were separated on a 10% SDS-PAGE and transferred to a PVDF membrane and MspA was detected with the polyclonal antiserum pAK MspA#813. The arrow indicates the location of the oligomeric form of MspA. Lane 1, 14 ng of protein extract from *M. smegmatis*; lane 2, 17  $\mu$ g of protein extract from *M. bovis* BCG (pSSa100); lane 3, 17  $\mu$ g of protein extract from *M. bovis* BCG (pMV306).

### 3.1.3 *M. bovis* BCG containing *mspA* shows an enhanced growth on plate

To investigate the influence of rMspA on growth of *M. bovis* BCG, in vitro growth experiments with *M. bovis* BCG (pSSa100) and *M. bovis* BCG (pMV306) were performed in Middlebrook broth and on Middlebrook plates. Both strains showed a similar growth rate in broth measured over a period of 6 weeks (data not shown). However, if the strains were plated on agar, a clearly enhanced growth of the *M. bovis* BCG derivative with the porin was noticed, which became apparent as an earlier appearance of colonies and a faster increase in colony size (Figure 4 A and C).

In order to quantify the growth differences between the two strains, the ATP content of colonies washed away from agar plates was measured. The *M. bovis* BCG derivative with rMspA always showed higher ATP amounts per 100 colonies than the reference strain. The growth advantage of *M. bovis* BCG (pSSa100) was reflected as two to four-fold higher cellular ATP-contents in different experiments (Figure 4 B and D). Thus, it was shown that the 3429 bp fragment from *M. smegmatis* transferred into *M. bovis* BCG ameliorated its growth on agar plates.

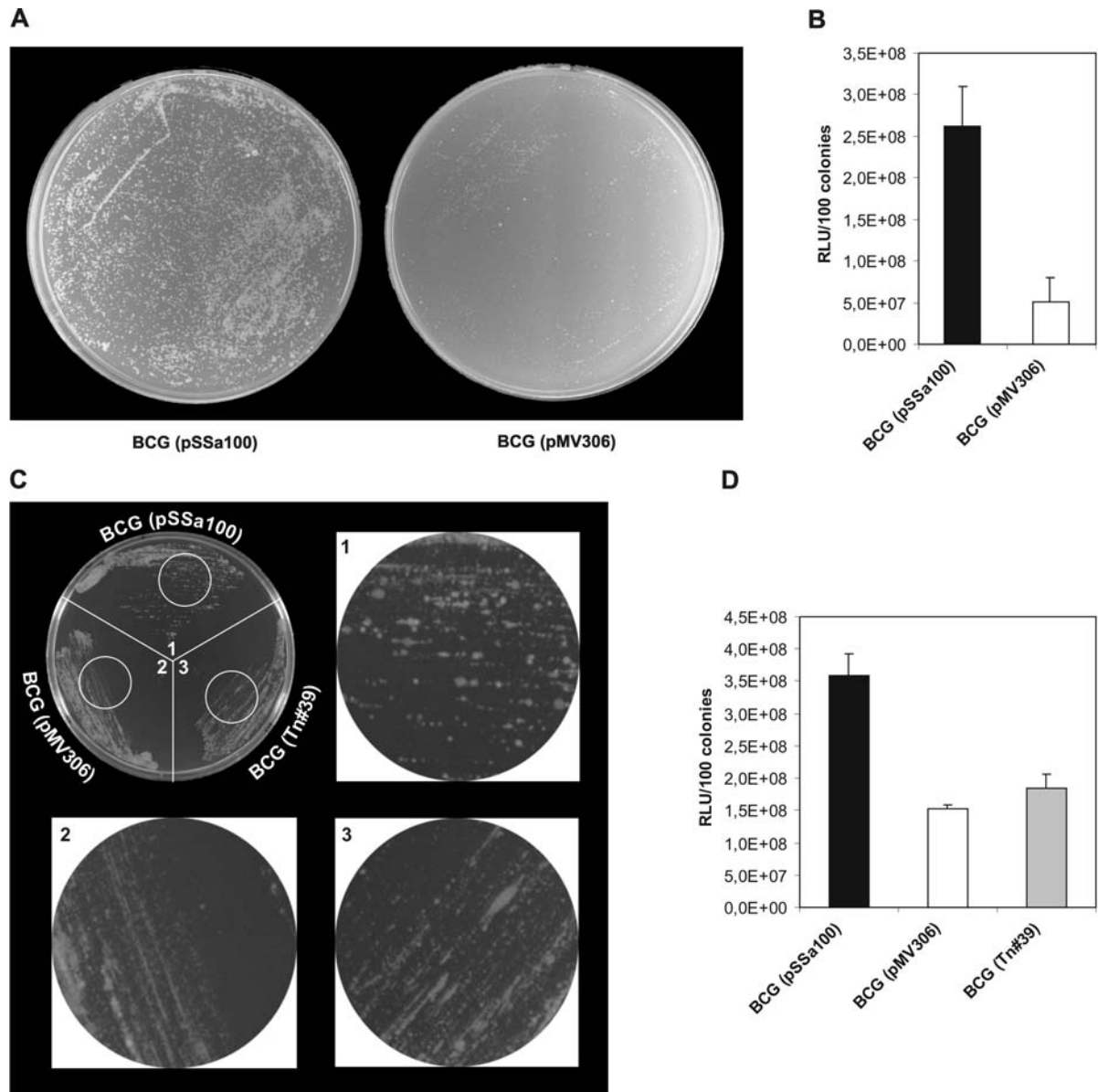


**Figure 4:** Enhanced growth of the *M. bovis* BCG derivative with rMspA on solid medium. A. Growth of the porin derivative *M. bovis* BCG (pSSa100) and the reference strain *M. bovis* BCG (pMV306) on Middlebrook agar plates 12 days after plating. B. Representative quantification of growth on plate by measuring the ATP content reflected as RLU in the luminescence assays. All values are standardized to 100 colonies. The *M. bovis* BCG derivative with rMspA showed up to four-fold higher cellular ATP concentrations if compared with the reference. C. Growth of *M. bovis* BCG (pSSa100), *M. bovis* BCG (pMV306) and *M. bovis* BCG (Tn#39, see section 4.1.4) streaked out on a Middlebrook agar plate. Sectors 1-3: Single colonies of *M. bovis* BCG (pSSa100) appeared after an incubation time of 16 days, whereas the reference and mutant strains showed either very small or no single colonies on plate. D. Effect of mutagenesis of *mspA* on growth on plates determined by representative quantification of the cellular ATP content. The *mspA* insertion mutant *M. bovis* BCG (Tn#39) showed comparable ATP concentrations as the reference, which were markedly lower than those of the *M. bovis* BCG derivative containing pSSa100.

### 3.1.4 Mutagenesis of *mspA* in pSSa100 reveals impairment of growth

Further proof that the *mspA* gene was responsible for the observed growth enhancement was adduced by transposon mutagenesis. The recombinant plasmid pSSa100 was mutagenized by an in vitro random insertion of a transposon with a tetracycline marker. A mutant with an insertion located in the coding sequence of *mspA* (Figure 2, Tn#39) was introduced into *M. bovis* BCG. The effect of the insertion on growth of *M. bovis* BCG on agar plates was measured by quantifying the ATP content of colonies containing the *mspA* gene with and without insertion. As shown in Figure 4 C and 4 D, the mutant strain *M. bovis* BCG (Tn#39) showed cellular ATP concentrations similar to the reference strain *M. bovis* BCG (pMV306), while *M. bovis* BCG (pSSa100) showed an enhanced growth. Hereby I demonstrated that the growth enhancement of *M. bovis* BCG (pSSa100) was caused by the introduced *mspA* gene.

### 3.1.5 Intracellular growth of *M. bovis* BCG containing the *mspA* gene

The intracellular growth of *M. bovis* BCG (pSSa100) and the reference strain was investigated by infection of non-activated J774A.1 macrophages and A549 pneumocytes by quantification of *M. bovis* BCG DNA via Real-time PCR. The *M. bovis* BCG strain with the recombinant porin showed in J774A.1 cells an initial growth phase until 56 hours post infection pronounced by a rapid increase of DNA (Figure 5 A). Until the end of the experiment the amount of intracellular *M. bovis* BCG (pSSa100) increased slightly. In contrast, the reference strain showed a delayed growth until 80 hours post infection with markedly lower amounts of intracellular bacteria. After 80 hours post infection a decline in measurable *M. bovis* BCG (pMV306) occurred (Figure 5 A).

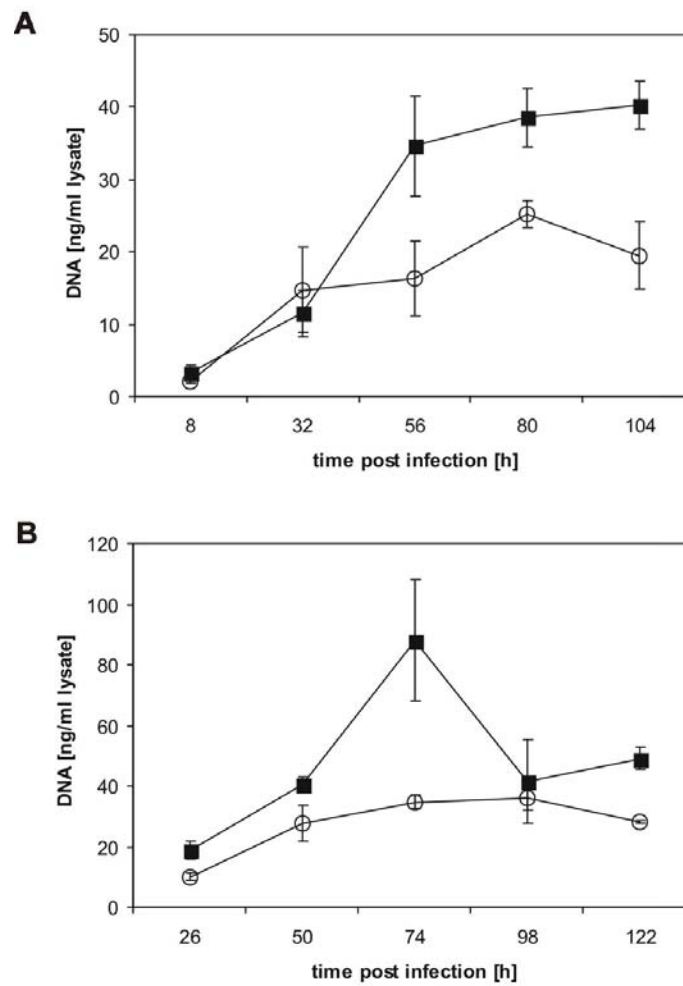


**Figure 5:** Representative measurement of intracellular growth of the *M. bovis* BCG derivative with rMspA and the reference strain. The DNA of intracellular bacteria was quantified by Real-time PCR. The closed squares demonstrate growth of *M. bovis* BCG (pSSa100) and the open circles growth of the reference *M. bovis* BCG (pMV306). Each value represents the mean ( $\pm$ SD) of DNA amounts from three independent experiments. A. Growth of *M. bovis* BCG derivatives in non-activated J774A.1. The values at 8 hours represent the amount of viable intracellular bacteria post infection. B. Growth of *M. bovis* BCG derivatives in the pneumocytic cells A549. The values at 26 hours represent the amount of viable intracellular bacteria post infection.

In the pneumocytic cells A549 an enhanced growth of intracellular *M. bovis* BCG (pSSa100) could be noticed if compared with the reference until 74 hours post infection (Figure 5 B). During the rest of the experiment a decline of intracellular *M. bovis* BCG (pSSa100) was detected. On the other hand the reference strain *M. bovis* BCG (pMV306) showed a very slow increase in bacterial amounts until 74 hours post infection followed by a declining phase (Figure 5 B).

These results indicate that *M. bovis* BCG containing the *mspA* gene shows an enhanced growth in monocytic and pneumocytic cells if compared with the reference.

### 3.2 Porins limit the intracellular persistence of *M. smegmatis*

To detect the potential impact of porins on survival in eukaryotic cells, I investigated the intracellular persistence of the wild type SMR5 and two porin deletion mutant strains of *M. smegmatis* MN01 ( $\Delta mspA$ ) and ML10 ( $\Delta mspA\Delta mspC$ ) in different models. *MspA* and *mspC* were chosen for deletions, since they are the only genes of this type of porin, which are expressed in the parental strain. After deletion of *mspA*, however, the homologous genes are expressed in the mutant strains (Dr. M. Niederweis, personal communication). Macrophages and amoebae were chosen as model systems to analyze intracellular survival.

#### 3.2.1 Intracellular persistence of *M. smegmatis* strains in macrophages

I began by investigating the degradation of *M. smegmatis* strains in J774A.1. As shown in Figure 6, a decrease in the number of intracellular mycobacteria was noticed during the course of the experiment. However, the double porin mutant ML10 showed significantly enhanced intracellular persistence when compared with the two other strains. After 54 h post infection SMR5 and MN01 showed bacterial loads of 2.7% and 3.4% when compared to bacterial loads after 6 h, whereas the bacterial load of J774A.1 infected with ML10 at 54 h amounted to 12.7%. The infection of BMMs produced more distinct differences between the three strains. ML10 exhibited throughout the entire experiment significantly higher CFU after plating when compared with the other two strains (Figure 6). After 30 h post infection, also BMMs infected with MN01 showed significantly higher bacterial loads than BMMs infected with SMR5. In BMMs infected with ML10, 18.7% of bacteria remained viable after 54 h as compared to the 6 h value. With respect to the other two strains, 16.8% of MN01 and only 3.7% of SMR5 were viable after 54 h (Figure 6).

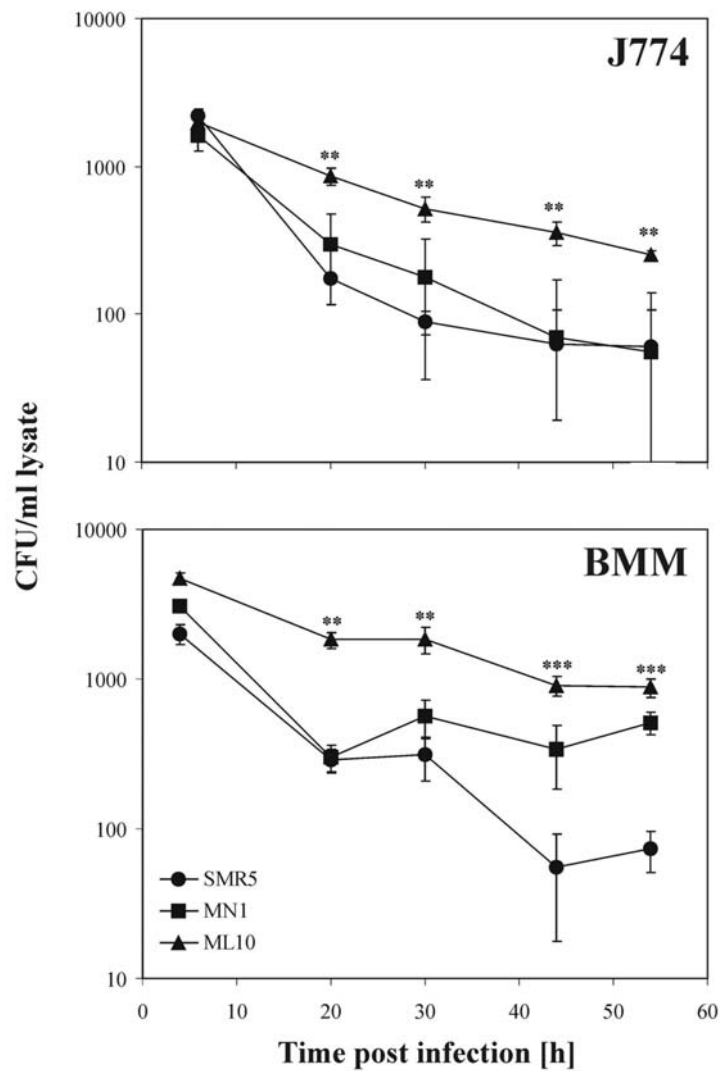


**Figure 6:** Intracellular persistence of *M. smegmatis* strains SMR5, MN01 and ML10 in J774A.1 and BMMs. Each value represents the mean ( $\pm$  SD) of three independent experiments. The values at 6 h represent the amount of viable intracellular *M. smegmatis* post infection. The double asterisks indicate values that varied significantly between ML10 and the other strains and the triple asterisks indicate significant differences among all three strains according to the paired Student's *t*-test ( $P < 0.001$ ).

### 3.2.2 Intracellular persistence of *M. smegmatis* strains in *A. castellanii*

*A. castellanii* was shown to serve as a host for mycobacteria such as *M. avium*. Additionally, *M. smegmatis* was reported to be killed by *A. castellanii* within a few days (Cirillo et al., 1997). Therefore, also this model was chosen to investigate intracellular persistence. As indicated in Figure 7 A, a pronounced initial killing phase occurred within the

first 20 h post infection. Afterwards the amount of intracellular ML10 did not decrease significantly while other strains showed a decline. While in *A. castellanii* infected with ML10 about 28% of bacteria remained intracellular and viable (relative to the 4 h values), MN01 and SMR5 showed levels between 5% and 0.66%, respectively (Table 4).

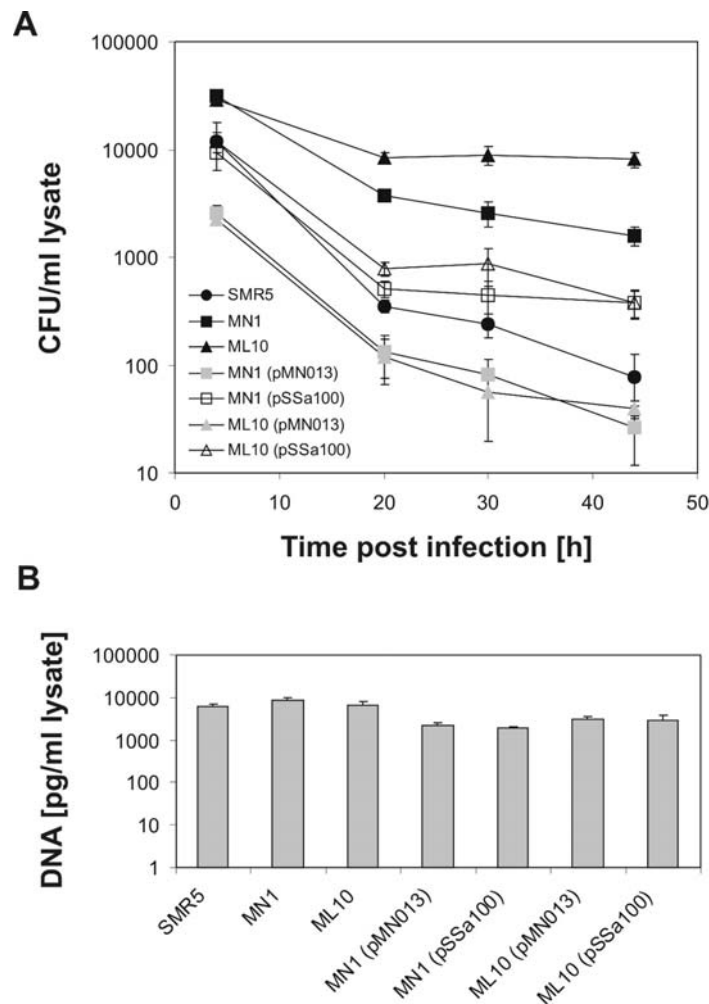


**Figure 7:** A. Intracellular persistence of *M. smegmatis* strains in *A. castellanii*. Each value represents the mean ( $\pm$  SD) of three independent experiments. The values at 4 h represent the amount of viable intracellular *M. smegmatis* post infection. B. Determination of consistent uptake of mycobacteria after 4 h post infection. DNA from intracellular mycobacteria was quantified by Real-time PCR. Columns show the mean ( $\pm$  SD) of three independent experiments.

To prove that the enhanced persistence of the mutants was in fact caused by the deletion of the porin genes, I performed complementation experiments by transforming the mutants with plasmids carrying the *mspA* gene. Plasmid pSSa100 (Figure 2) carries a 3.4 kb

DNA fragment from *M. smegmatis* containing the *mspA* gene with its own promoter in an integrative vector, while plasmid pMN013 (see appendix) carries the *mspA* gene fused to the *M. smegmatis* promoter p<sub>imyc</sub> on a shuttle vector. The intracellular persistence of the mutants carrying either pSSa100 or pMN013 was tested in *A. castellanii*, because the differences between the mutants were most pronounced in this test system. As shown in Figure 7 A and Table 5, complementation of the porin deletion in mutant strains was achieved by introducing pMN013 as well as pSSa100. While complementation of porin deletion by pMN013 resulted in a higher *mspA* expression in both mutant strains than in the parental strain, complementation by pSSa100 was only partial (Table 5). Transfer of pSSa100 only provides one copy of *mspA* to the recipients and *mspA* is under control of its own promoter. The shuttle plasmid pMN013 is present in several copies in mycobacteria and the promoter p<sub>imyc</sub> is a relatively strong promoter (Kaps et al., 2001).

**Table 4:** Bacterial load in *A. castellanii* infected with *M. smegmatis* strains. Values demonstrate the percentage of viable intracellular mycobacteria at 44 h post infection when compared to the 4 h values.

Strains	Intracellular persistence after 44h
SMR5	0.66%
MN01	5.0%
ML10	28.1%
MN01 (pMN013)	1.0%
MN01 (pSSa100)	4.0%
ML10 (pMN013)	1.8%
ML10 (pSSa100)	3.1%

RT-Real-time PCR experiments confirmed a much stronger expression of *mspA* from pMN013 compared to pSSa100 (Table 5). Transcription of *mspA* in the mutants carrying pMN013 was about 7 to 10 times stronger than in wild type. Nevertheless, both plasmids affected an adaptation towards the phenotype of the wild type SMR5 (Figure 7A). The complemented strains with pSSa100 were degraded similar to the wild type up to 20 h post infection. However, after this point of time, their number remained relatively constant until the end of the experiment. MN01 (pMN013) and ML10 (pMN013) were degraded more efficiently by *A. castellanii* than all the other tested strains including SMR5. The decrease of

the intracellular persistence of the mutants harboring either pSSa100 or pMN013 confirmed that the deletion of the porin genes was responsible for the enhanced persistence of the mutants in the amoeba (Figure 7 A).

**Table 5:** Porin expression in the wild type, deletion mutants and complemented strains. Values represent the quantification of porin mRNA, reflected as cDNA, measured via RT-Real-time PCR. Data are the means ( $\pm$  SD) of three measurements.

Strains	Porin expression [pg cDNA / ng RNA]	% of porin expression referring to SMR5
SMR5	15.76 $\pm$ 4.89	100
MN01	0.36 $\pm$ 0.02	2.3
ML10	0.82 $\pm$ 0.17	5.2
MN01 (pMN013)	144.43 $\pm$ 10.89	916.3
MN01 (pSSa100)	2.90 $\pm$ 0.12	18.4
ML10 (pMN013)	111.38 $\pm$ 20.80	706.6
ML10 (pSSa100)	1.73 $\pm$ 0.56	11.0

Although all strains were applied at an MOI of 10, the CFU values of the first samples taken 4 h after infection already diverged, which is consistent with a kill off of mycobacteria by the amoebae starting directly after phagocytosis. Cirillo et al. (1997), for example, reported that 30 min after entry of *M. smegmatis* into *A. castellanii* the majority of bacteria were partially degraded. To ensure that equal numbers of bacteria of all strains had been taken up by the amoebae, the DNA of intracellular *M. smegmatis* after the initial infection time was quantified. There was no significant difference in the amount of intracellular DNA of all tested strains at 4 h post infection (Figure 7 B).

So far few studies have been performed, which illustrate the intracellular persistence of mycobacteria in *A. castellanii* particularly with regard to *M. smegmatis*. Therefore, I also examined the infection of *A. castellanii* with the wild type SMR5, MN01 and ML10 by means of transmission electron microscopy of samples taken after 18 h (Figure 8), 30 h (Figure 9) and 42 h (data not shown) post infection. Phagosomes were detected containing intact bacteria as well as degradation products up to 42 h post infection. Most of the phagosomes contained more than one *M. smegmatis* (typically up to 15), as indicated by the arrows in Figure 8 and 9.

At 18 h post infection the wild type SMR5 showed incipient degradation (see arrowhead in Figure 8 B), whereas less detritus was observed in phagosomes containing the porin deletion mutants (Figure 8 C and D). However, increased degradation was observed over the course of infection (Figure 9 B-D).

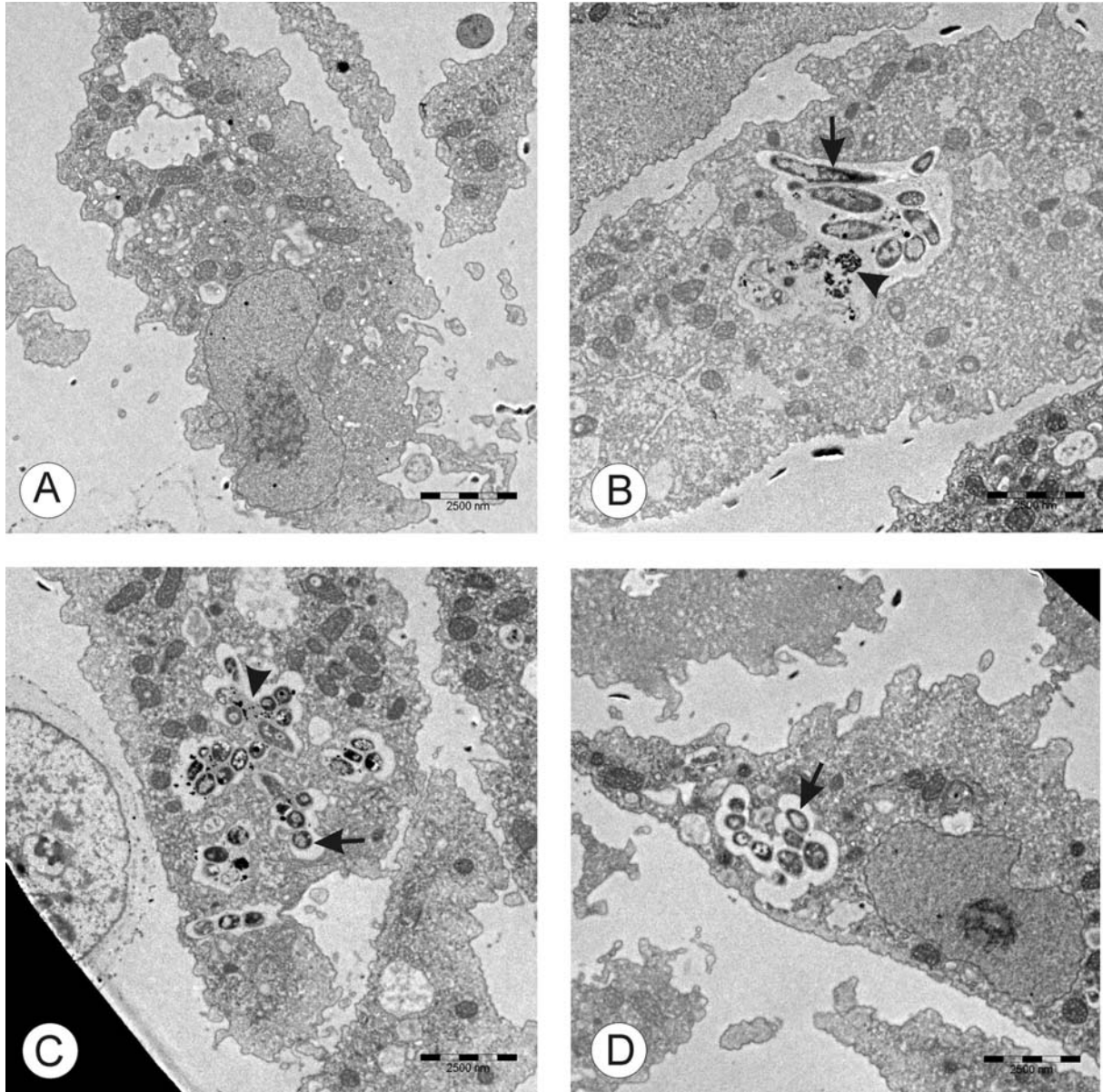


**Figure 8:** TEM of cultured *A. castellanii* 18 h post infection. A. Non-infected control. B. Infected with *M. smegmatis* SMR5 (wild type). C. Infected with *M. smegmatis* MN01 ( $\Delta mspA$ ). D. Infected with *M. smegmatis* ML10 ( $\Delta mspA\Delta mspC$ ). Arrows indicate *M. smegmatis*, whereas detritus is indicated by arrowheads.

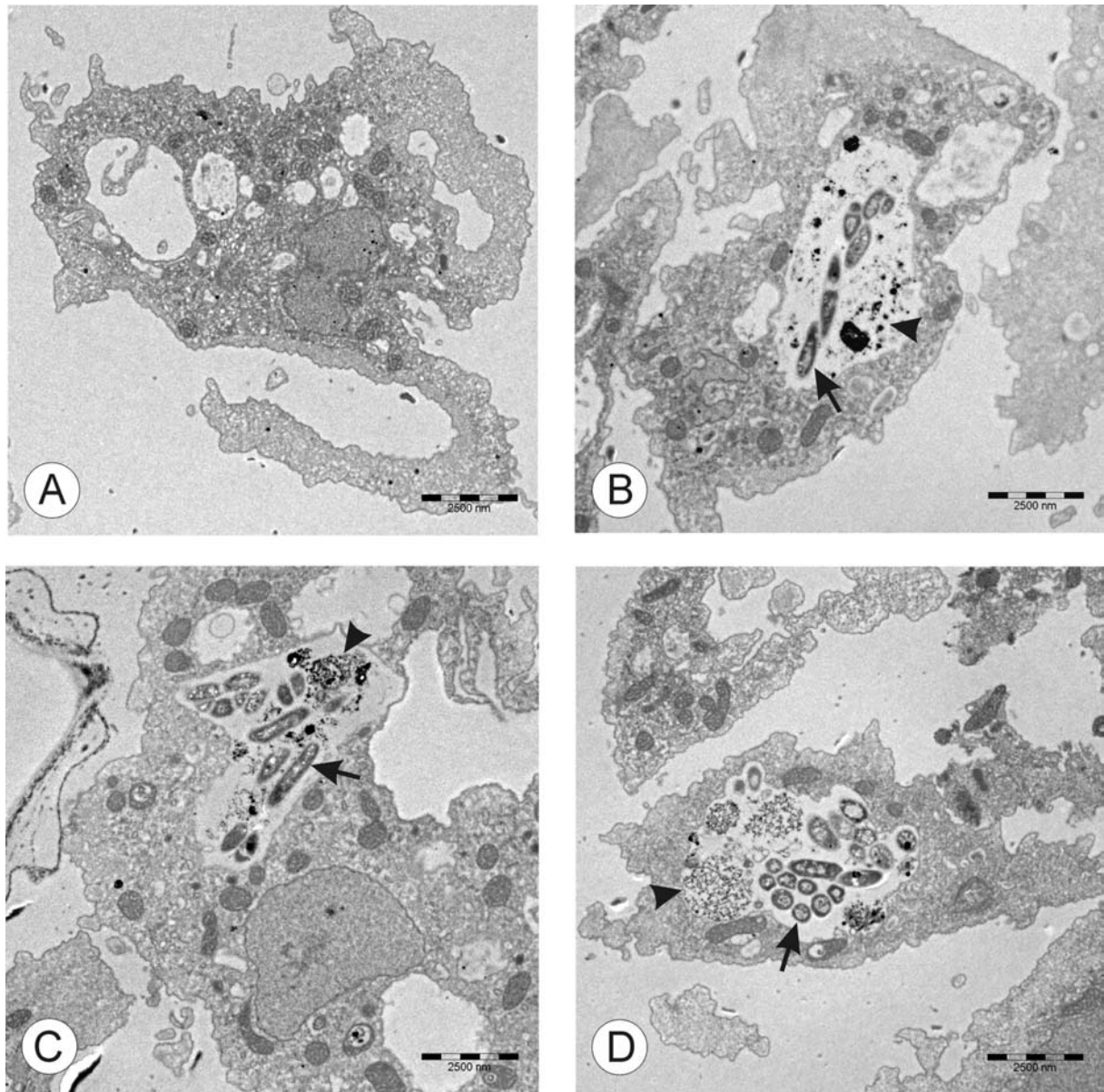


**Figure 9:** TEM of cultured *A. castellanii* 30 h post infection. A. Non-infected control. B. Infected with *M. smegmatis* SMR5 (wild type). C. Infected with *M. smegmatis* MN01 ( $\Delta mspA$ ). D. Infected with *M. smegmatis* ML10 ( $\Delta mspA\Delta mspC$ ). Arrows indicate *M. smegmatis*, whereas detritus is indicated by arrowheads.

It should be noted that after 30 h post infection some trophozoites rounded up and encystment of *A. castellanii* was observed. Electron micrographs revealed double-walled cysts. *M. smegmatis* was not only present in phagosomes but also was found to be embedded in walls of cysts of *A. castellanii* (Figure 10).

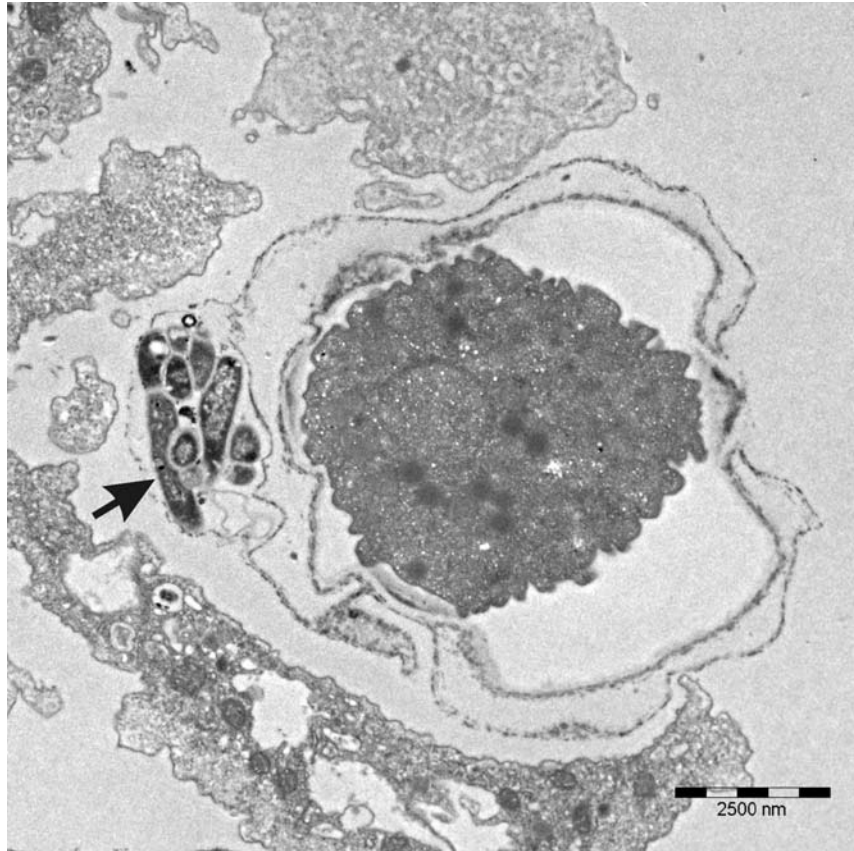


**Figure 10:** TEM of amoeba cyst including mycobacteria (*M. smegmatis* MN01) in the cyst wall as indicated by the arrow.

### 3.2.3 Growth of *M. smegmatis* strains in broth culture at different pH

As the double mutant lacking *mspA* and *mspC* exhibited an enhanced survival in phagocytes, the question arose, if this was caused by an improved resistance to acidic pH conditions present in the phagosomes. To answer this question, the growth of SMR5, MN01 and ML10 were compared in Middlebrook 7H9 medium at pH 6.7 and pH 5.0 over 8 days. The double mutant strain ML10 exhibited a decreased growth at pH 6.7 and pH 5.0 across the course of the experiment when compared with SMR5 and MN01 (Figure 11). No significant differences were noticed between the growth of SMR5 and MN01. The differences in the growth rates in broth culture between the three strains were independent of the pH of the medium.

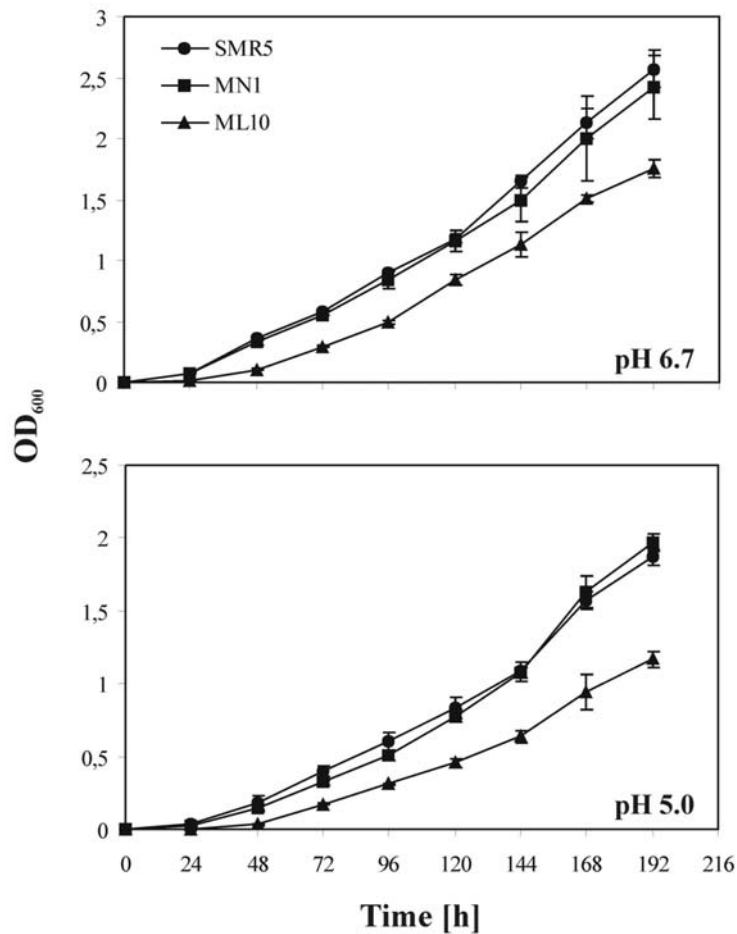


**Figure 11:** Impact of porin deletions on growth of *M. smegmatis* under different pH-conditions. The strains were grown in Middlebrook 7H9 at pH 6.7 or pH 5.0. Measuring points represent the mean ( $\pm$  SD) of three independent cultures.

### 3.3 Characterization of porins from members of the *M. fortuitum*-group

Since the saprophytic bacterium *M. smegmatis* causes disease only in rare cases (Brown-Elliott & Wallace, 2002), it is important to investigate the role of porins on virulence in more pathogenic members of RGM. Members of the *M. fortuitum*-group were therefore chosen to detect and analyze homologous porins of the *mspA* class. For this purpose, two different *M. fortuitum* strains (10851/03 & 10860/03) and two *M. peregrinum* strains (9912/03 & 9926/03) were employed, which originally were isolated from human patients and were provided by the National Reference Center for Mycobacteria at the Research Center Borstel, Germany. Comparative analysis was performed using also the type strain *M. fortuitum* DSM 46621. In order to verify the taxonomic classification and to define the phylogenetic relationship

between the named strains or species, complete sequences of the 16S rRNA genes were determined using the primers, which were approved by Adekambi & Drancourt (2004). As shown in Figure 14, phylogenetic analysis of the 16S rRNA sequences confirmed the taxonomic classification of the employed members of the *M. fortuitum*-group.

### 3.3.1 *PorM1* is present in different members of the *M. fortuitum*-group

To detect porins homologous to *mspA* in members of the *M. fortuitum*-group, hybridization experiments were performed with a probe derived from preliminary porin gene sequences of *M. fortuitum*. Preliminary porin gene sequences from *M. fortuitum* were obtained by performing PCRs under low stringency conditions using primers derived from the *mspA* sequence. The probe hybridized to the genomic DNA from the *M. fortuitum* strains as well as to the genomic DNA from *M. peregrinum* strains. Thus, homologous porins seem to exist in all strains. The probe hybridized to two fragments of the *Sac*II-digested genomic DNA of *M. fortuitum* and *M. peregrinum*. However, the fragment sizes differed among the members of the *M. fortuitum*-group (Figure 12). Hence, the *M. fortuitum* and *M. peregrinum* genomes contain at least two copies of the porin gene.

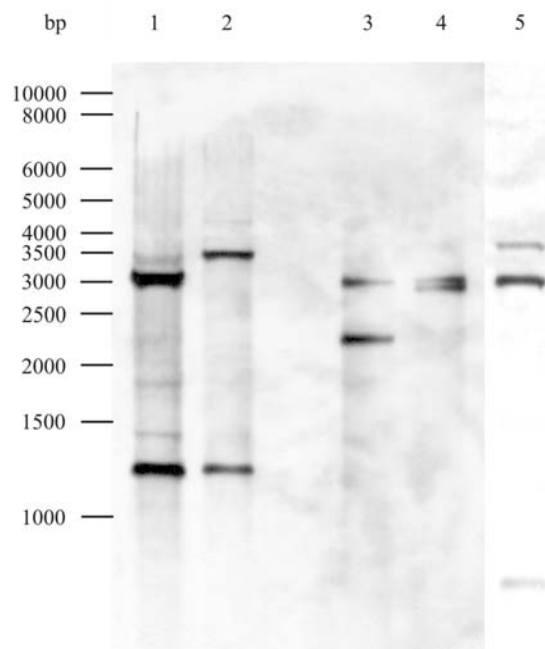


**Figure 12:** Occurrence of porin genes among members of the *M. fortuitum*-group. Chromosomal DNA of different strains was digested with *Sac*II and analyzed by Southern blotting. Lanes: 1, *M. peregrinum* 9912/03; 2, *M. peregrinum* 9926/03; 3, *M. fortuitum* 10851/03; 4, *M. fortuitum* 10860/03; 5, *M. fortuitum* DSM 46621.

### 3.3.2 *PorM1* genes from members of the *M. fortuitum*-group are highly homologous to *mspA*

To clone porins from *M. fortuitum*, genomic DNA of *M. fortuitum* 10860/03 was digested with SacII and a 3000 bp fragment was cut out of the preparative gel. The DNA was ligated into the unique SacII site of pIV2 and transformed into *E. coli*. After screening the transformants by Dot Blot analysis, two clones were identified to contain porin sequences, from which the plasmids pSSp107 and pSSp108 were isolated. Both plasmids turned out to contain the same genomic region of 2895 bp including one porin gene and were chosen for further characterization. The inserts were sequenced by primer walking, whereas both strands of the porin genes and their surrounding regions were sequenced twice at least. As shown in Figure 13, the insert of the plasmids contained several ORFs, one of which (*porM1*) was homologous to *mspA*. It contained 636 bp, encoding a protein of 211 amino acids with an N-terminal signal sequence of 27 amino acids, which was predicted using the SignalP 3.0 Server at <http://www.cbs.dtu.dk/services/SignalP/> (Bendtsen et al., 2004).

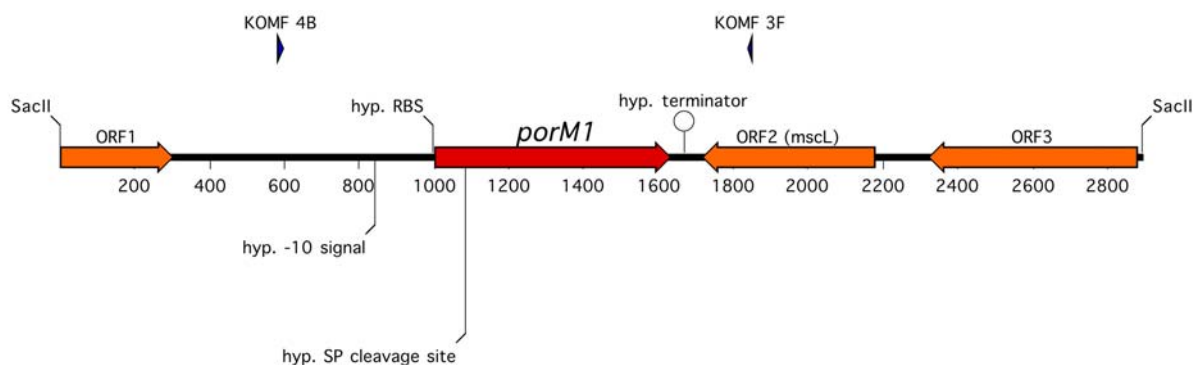


**Figure 13:** Map of the insert of plasmid pSSp107. The insert includes the *porM1* gene and three other ORFs. Up- and downstream to *porM1* various nucleotide signal sequences were detected: -10 signal of a promoter (TATGTT), a ribosome binding site (RBS: GGAGA), a signal peptide (SP) of 81 bp and a hairpin structure, which could represent a terminator. The binding sites of the primers used for detection of the genomic regions of *porM1* in other employed strains are indicated as KOMF 4B and KOMF 3F.

A hypothetical -10 region of a promoter and a ribosome binding site (RBS) were identified upstream of the coding sequence. Downstream of the ORF an inverted repeat was detected, which could function as a terminator by forming a hairpin structure (Figure 13). It has to be noted that the sequence homology between *M. fortuitum* and *M. smegmatis* was restricted to the coding sequence. According to the designation of other mycobacterial porin

genes and to the instructions of EMBL nucleotide sequence database, the gene was named *porM1*.

Besides the porin gene two other complete ORFs and a part of another ORF were detected. ORF1 was interrupted by one of the SacII sites and showed a high homology to a molybdopterin biosynthesis protein of *M. tuberculosis* CDC 1551 (GenBank Accession-Nr.: AAK45260). ORF2 turned out to be a mechanosensitive channel homologous to the gene *mscL* from *M. avium subsp. paratuberculosis* str. 10 (GenBank Accession-Nr.: NP959854). ORF3 was homologous to the hypothetical protein Rv0990c from *M. tuberculosis* H37Rv (GenBank Accession-Nr.: NP215505).

Next it had to be answered, whether *porM1* was present in other employed strains. Thus, the primers KOMF3F and KOMF4B were chosen to amplify a fragment of approximately 1250 bp including the porin gene and flanking regions. PCRs, using a polymerase-mix with proofreading activity, revealed the specific fragment to be present in all strains. Several PCRs were performed and both strands of the different fragments were sequenced. *PorM1* was detected in all members of the *M. fortuitum*-group and the nucleotide sequences were submitted to the EMBL nucleotide sequence database (Table 6). The nucleotide sequences are given in the section Appendix. The nucleic acid subsequences such as the -10 signal of a promoter, the RBS, the signal peptide of 81 bp and the hairpin structure were also present and were conserved among all tested strains (data not shown).

**Table 6:** Nucleotide sequence homology between *porM1* from members of the *M. fortuitum*-group and *mspA*.

Species	Nucleotide similarity index	Accession-nr. to the EMBL nucleotide sequence database
<i>M. fortuitum</i> DSM 46621	88.2%	AJ880097
<i>M. fortuitum</i> 10851/03	88.4%	AJ880098
<i>M. fortuitum</i> 10860/03	87.4%	AJ874299
<i>M. peregrinum</i> 9912/03	86%	AJ880099
<i>M. peregrinum</i> 9926/03	86.9%	AJ880100

As already indicated in Table 6, the nucleotide sequences of the gene *porM1* differed among members of the *M. fortuitum*-group. The phylogenetic comparison of the employed strains based on their porin sequences showed the closest relationship between the type strain *M. fortuitum* DSM 46621 and *M. fortuitum* 10851/03. It could, however, not reflect the phylogenetic relationships among the *M. fortuitum*-group based on 16S rRNA sequences (Figure 14).

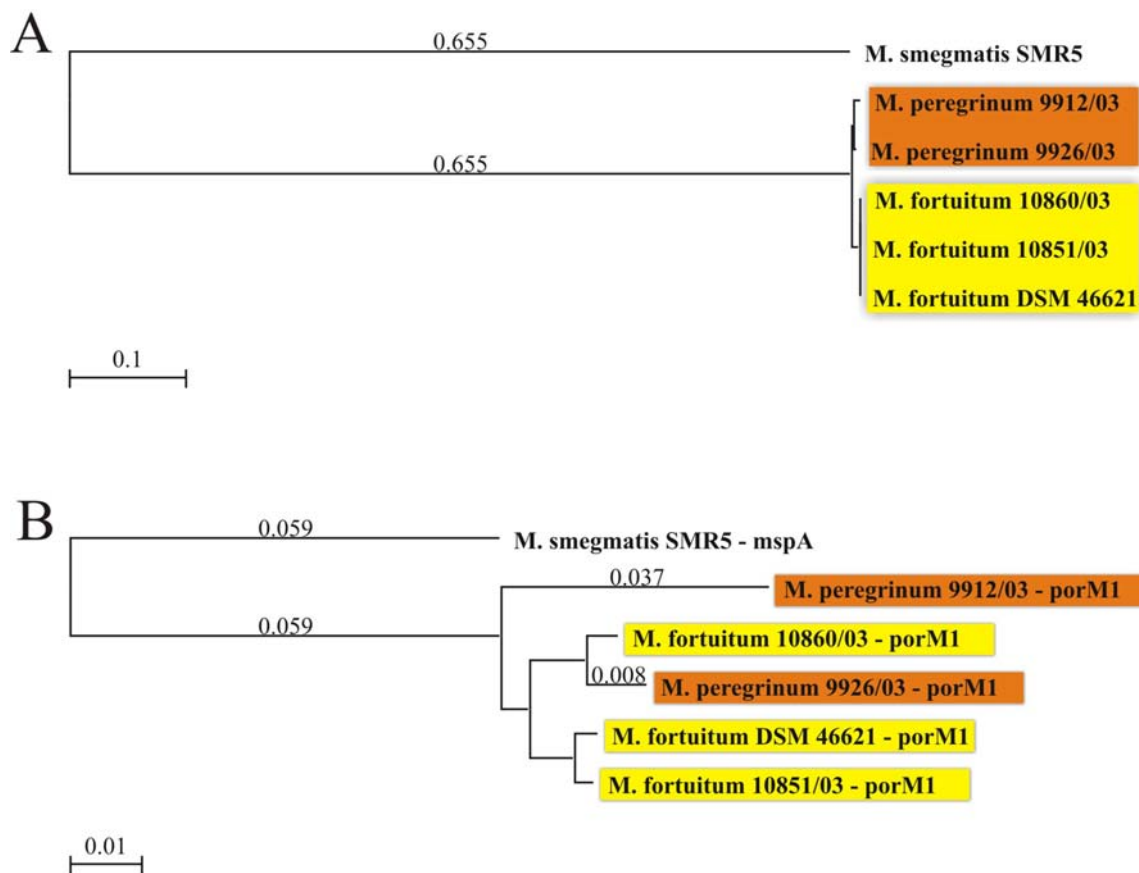


**Figure 14:** Phylograms of the *M. fortuitum*-group based on 16S rRNA and *porM1* sequences using the neighbor-joining method with Kimura 2-Parameter distance correction. The branch lengths indicate the evolutionary distance relative to the scale. *M. smegmatis* was used as the outgroup. All *M. fortuitum* strains are shaded yellow and the *M. peregrinum* strains are shaded orange. A. Phylogenetic tree of 16S rRNA gene sequences of employed mycobacteria. B. Phylogenetic tree of porin gene sequences of employed mycobacteria.

The amino acid sequences of PorM1 among the *M. fortuitum*-group were, however, highly conserved (Figure 15). All *M. fortuitum* strains possessed 100% identical PorM1 amino acid sequences, whereas *M. peregrinum* 9926/03 exhibited only one and *M. peregrinum* 9912/26 only two amino replacements compared to the sequence from *M. fortuitum*. According to studies about typical amino acid substitutions in conserved proteins by Betts & Russell (2003), all amino acid replacements were exchanges between amino acids, which are preferred for membrane proteins. The aliphatic and hydrophobic amino acid Isoleucine was substituted with the similar aliphatic and hydrophobic amino acid Leucine.

The negatively charged and polar amino acid Glutamate was replaced by the negatively charged (and very similar) amino acid Aspartate.

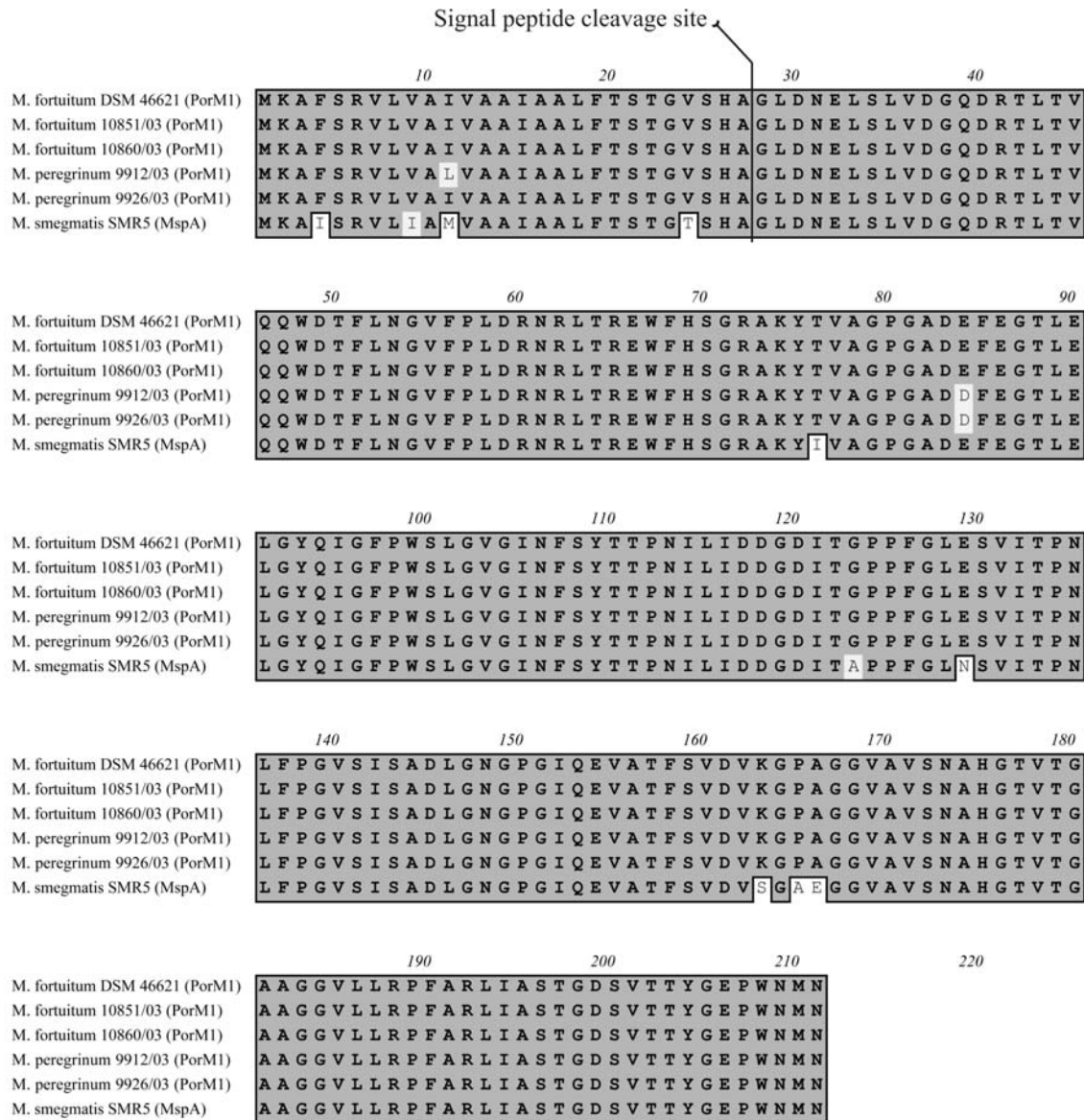


**Figure 15:** Alignment of PorM1 from members of the *M. fortuitum*-group and MspA. The start codon ATG and the stop codon TGA were chosen according to the sequence of *mspA*. The cleavage recognition site of the signal peptidase was predicted for PorM1 using the SignalP 3.0 Server at <http://www.cbs.dtu.dk/services/SignalP/> (Bendtsen et al., 2004). The predicted signal peptide cleavage sites corresponded to those from MspA. Identical amino acids are shaded in dark gray, similar amino acids are shaded in light gray and different amino acids are non-shaded.

---

The amino acid sequences of porins from members of the *M. fortuitum*-group and *M. smegmatis* were also highly conserved. The mature proteins (without signal peptide) possessed 97.3% similar and at least 96.2% identical amino acids (Betts & Russel, 2003).

### 3.3.3 PorM1 is expressed in the members of the *M. fortuitum*-group

The expression of the porin *porM1* and detection of the mature oligomeric porin was examined by SDS-PAGE, 2D-Electrophoresis and Western blotting. Therefore, protein was isolated from *M. fortuitum* 10860/03 using the detergent nOPOE and separated by 2D-Electrophoresis. As shown in Figure 16 A, about 50 protein spots were detected on the 2D-gel. Western blot experiments with identical gels showed only one defined spot detected by the antiserum pAK MspA#813 (Figure 16 A I). The protein had an apparent molecular mass of approximately 120 kDa and an apparent isoelectric point (Ip) of about 4, which corresponded well to the predicted Ip of the mature protein of 4.1.

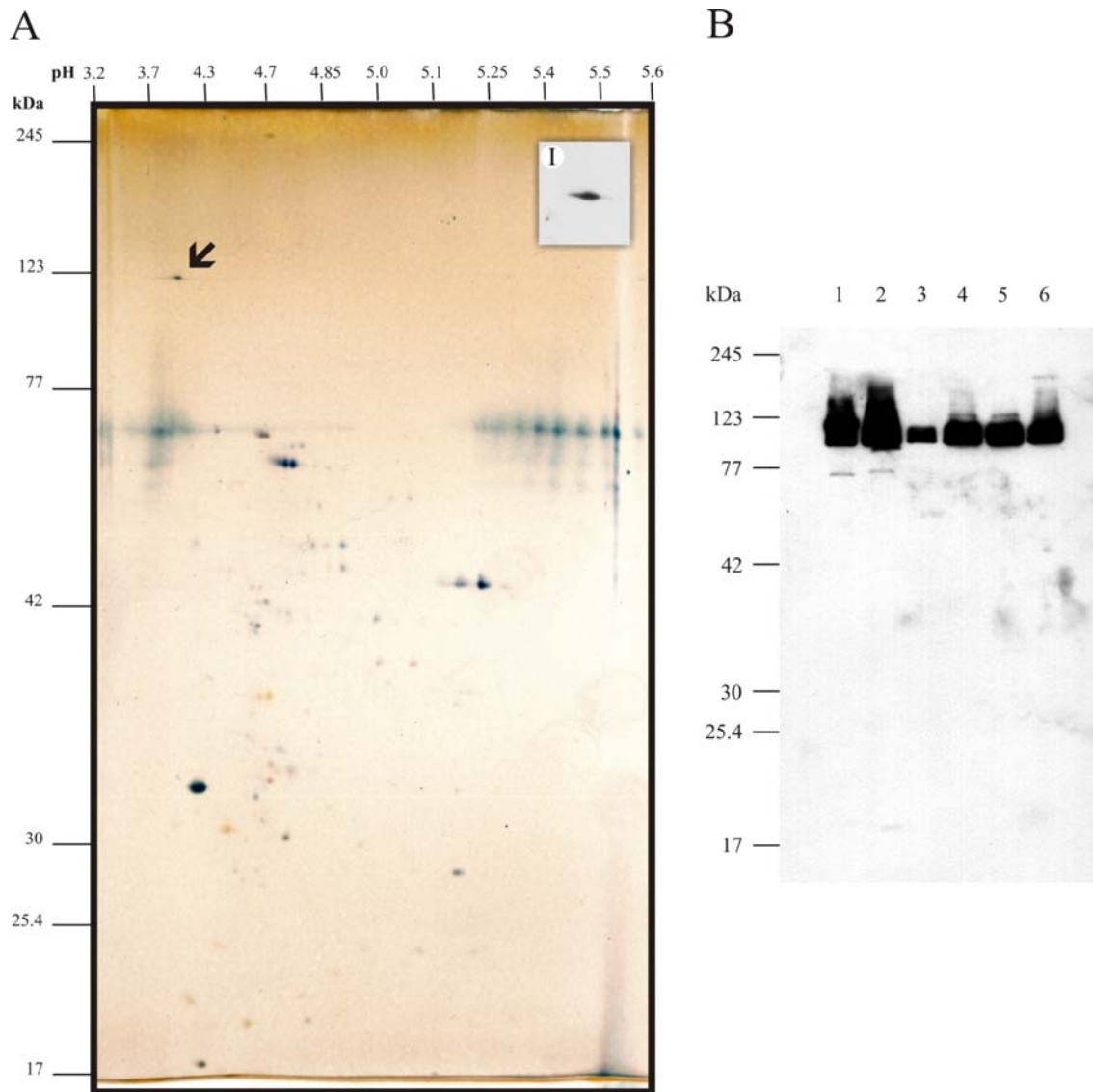


**Figure 16:** Detection of PorM1 in members of the *M. fortuitum*-group. 2D-Electrophoresis and Western blot experiments proved PorM1 to be expressed in the analyzed strains. A. 2D-Electrophoresis of protein isolation from the strain *M. fortuitum* 10860/03 using the detergent nOPOE. The arrow indicates the porin spot as proved by Western blot analysis (see section I). B. Detection of the porin in members of the *M. fortuitum*-group by Western blotting. 10-30  $\mu\text{g}$  of protein was detected by the antiserum pAK MspA#813. Lanes 1-6: 1, *M. smegmatis* SMR5 (10  $\mu\text{g}$ ); 2, *M. fortuitum* DSM 466211 (30  $\mu\text{g}$ ); 3, *M. fortuitum* 10851/03 (30  $\mu\text{g}$ ); 4, *M. fortuitum* 10860/03 (30  $\mu\text{g}$ ); 5, *M. peregrinum* 9912/03 (30  $\mu\text{g}$ ); 6, *M. peregrinum* 9926/03 (30  $\mu\text{g}$ ).

Since the oligomeric porin was detected in cell extracts of *M. fortuitum* 10860/03 (Figure 16 A), other members were tested for expression of PorM1. The mature oligomeric form of the porin was shown in cell extracts of the members of the *M. fortuitum*-group as well as in extracts from *M. smegmatis*, which served as a positive control (Figure 16 B). After extended exposition times also the monomeric form of the porin was detected on Western

blots (data not shown). Although equal amounts (30 µg) of the cell extracts from members of the *M. fortuitum*-group were blotted on the PVDF membrane, the signals on the Western blots and thus the amount of PorM1 seemed not to be equal among the tested strains (Figure 16 B).

### 3.3.4 Members of the *M. fortuitum*-group express less porin than *M. smegmatis*

The disparate signal intensities on Western blot experiments among the *M. fortuitum*-group gave rise to analyze the expression profile of *porM1*. For this purpose, cell extracts with the detergent nOPOE were employed in ELISA experiments to quantify the amount of porin in different strains. Furthermore, the expression of *porM1* in the members of *M. fortuitum*-group was determined by means of RT-Real-time PCR using sequence specific primers and probes and was compared to porin expression in *M. smegmatis*.

Different dilutions of the cell extracts from the various strains were loaded to the wells of a microtitre plate and porins were detected by an antiserum raised against MspA (pAK MspA#813). Higher amounts than 5 µg per well turned out to be inapplicable due to saturation effects and the detection of porin in cell extracts failed at concentrations of about 0.04 µg per well (Figure 17 A). Therefore, the most eligible working range turned out to be 1 µg cell extract per well. Indeed, the amount of porin differed in various strains. The highest amount of porin was detected in the internal control *M. smegmatis* SMR5. The type strain *M. fortuitum* DSM 46621 exhibited porin amounts close to *M. smegmatis*, whereas all of the strains, which originally were isolated from human patients showed clearly decreased porin amounts (Figure 17 A). I observed with particular interest the amount of porin in *M. fortuitum* 10851/03, which showed the lowest amount among the analyzed RGM. Since *M. bovis* BCG does not possess homologous porins (Niederweis et al., 1999), extracts of *M. bovis* BCG were employed to detect the background. Figure 17 A demonstrates that the antibody specifically recognized MspA and the homologous porin PorM1.

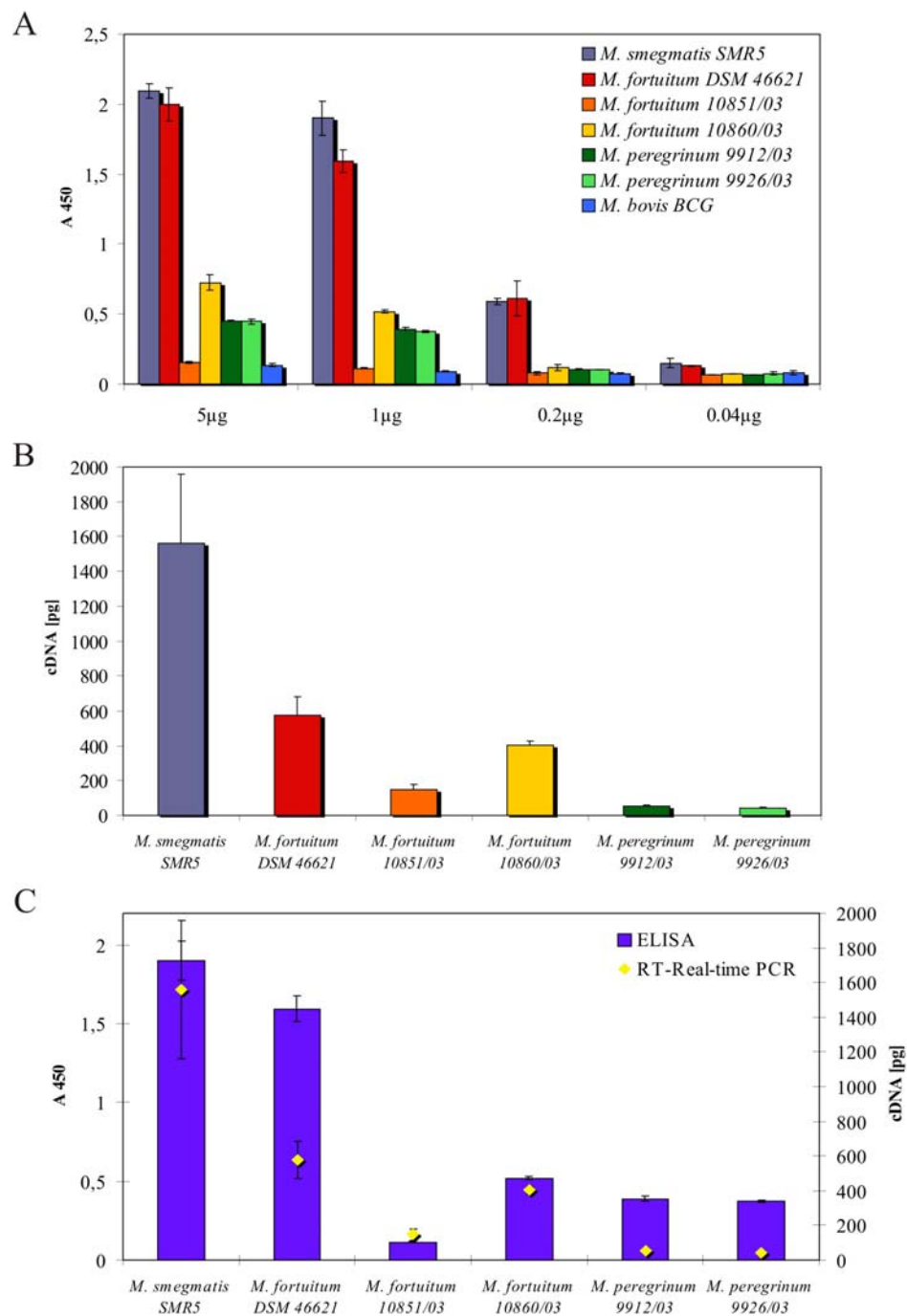


**Figure 17:** Comparative analysis of porin expression among RGM. Expression of porin was detected by means of ELISA and RT-Real-time PCR. Each value represents the mean ( $\pm$ SD) of at least three independent experiments. A. Quantification of porin in cell extracts of different mycobacteria using the polyclonal antibody pAk MspA#813. B. Quantification of porin transcription in various RGM using specific primers and probes for *mspA* or *porMI*, respectively. C. Combined illustration of the results from ELISA- and RT-Real-time PCR-experiments. The left ordinate and the blue columns demonstrate the results from ELISA-experiments using 1 µg protein per well, whereas the right ordinate and the yellow rhombs show the results from RT-Real-time PCR-experiments.

Comparative expression analysis was also performed by means of RT-Real-time PCR using specific primers and probes for *porM1* or *mspA*, respectively. 100 ng of RNA preparations from RGM were employed to compare the transcription of the porin genes among the strains. As it was already proven by the ELISA-results, the highest porin transcription was measured in *M. smegmatis*. It showed about twice as high transcription rates as the highest transcription rate among the *M. fortuitum*-group, which belonged to the type strain *M. fortuitum* DSM 46621. *M. fortuitum* 10851/03 exhibited the lowest transcription rate among all *M. fortuitum* strains, whereas the two *M. peregrinum* strains showed even lower amounts of porin mRNA than any other tested strain (Figure 17 B). The combined illustration (Figure 17 C) of the amounts of *porM1* protein and mRNA isolated from various strains demonstrates the clear concordance of transcription rates with translation rates of porin genes among the RGM.

These results show that although the amino acid sequences of porin genes among the RGM are highly conserved, the expression profiles of porins differ even among the strains of one species.

### 3.3.5 PorM1 is exposed to the surface of *M. fortuitum*

MspA was shown to be accessible on the cell surface of *M. smegmatis* by using the antiserum pAK MspA#813 (Stahl et al., 2001). Since the expression analysis showed a decreased amount of porin in members of the *M. fortuitum*-group, *M. fortuitum* DSM 46621 and *M. fortuitum* 10860/03 (the two strains with the highest porin expression rates) were exemplary employed for detection of porins at the surface of intact mycobacteria. I first started with detection of porins at the surface of *M. fortuitum* by means of flow cytometry experiments, however, no MspA-specific signal was measured compared to the autofluorescence of untreated mycobacteria (data not shown). Thus, the detection of the primary MspA-specific antibody was performed by using a secondary horseradish peroxidase conjugated anti-rabbit IgG in quantitative microwell immunoassays. Every molecule of peroxidase catalyzes the oxidation of many molecules of substrate, which results in amplification of the signal and in turn in a higher sensitivity of the assay compared to flow cytometry experiments. As shown in Figure 18, porins were accessible at the surface of intact cells of *M. fortuitum* and were detected by the porin specific antibody. Significantly higher absorption at 450 nm was measured for *M. fortuitum* DSM 46621 as well as *M. fortuitum*

10860/03 compared to the relative backgrounds, which were measured by applying only the secondary antibody and measuring its non-specific binding.

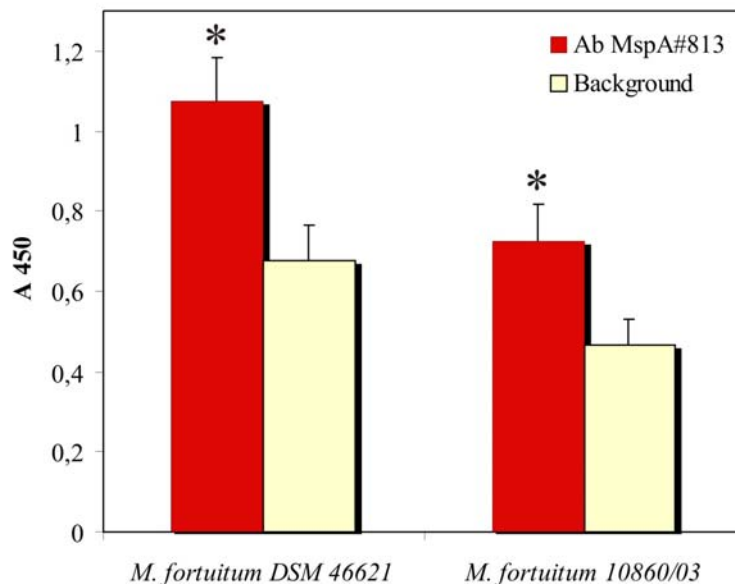


**Figure 18:** Detection of PorM1 at the surface of *M. fortuitum* using the porin-specific antiserum pAK MspA#813 in quantitative microwell immunoassays. Each column represents the mean ( $\pm$ SD) of 8 measurements. Asterisks indicate significant differences between the samples, which were treated with pAK MspA#813 and backgrounds according to the paired Student's *t*-test ( $P < 0.001$ ).

The ratio of detected porin at the surface between the two strains was consistent with ratios, which were obtained by analyzing the expression profiles (see above). Because of this finding and because *M. smegmatis* expresses higher levels of porin (Figure 17 C), the density of porins in the OM of members of the *M. fortuitum*-group is probably lower than in the OM of *M. smegmatis*.

### 3.4 Construction of the suicide plasmid pSSs003

As a consequence of at least eight *Mycobacterium* genome-sequencing projects, which are at or near completion, plenty of sequence data is provided, which remains to be functionally characterized. Identification and characterization of new genes, however, requires in many cases the mutagenesis of genes and study of phenotypes of the mutant strains. I therefore constructed a suicide plasmid suitable for mutagenesis of any mycobacterial gene with known nucleotide sequence. There are few appropriate and functional resistance genes, which are qualified for mycobacteria. One of those is the *hyg*

resistance gene, which was applied to construct pSSs003. This plasmid provides two multiple cloning sites for cloning of flanking regions from target genes to enable allelic exchange between the target sequence and the *hyg* gene by homologous recombination. The inserted fragments can be verified by the two sequencing primers *hygseq\_1* (5'-TCG CCT TCA CCT TCC TGC-3') and *hygseq\_2* (5'-GTA ACA GGG ATT CTT GTG TCA C-3'), which allow sequencing reactions at an annealing temperature of 54°C (Figure 19 and 20).

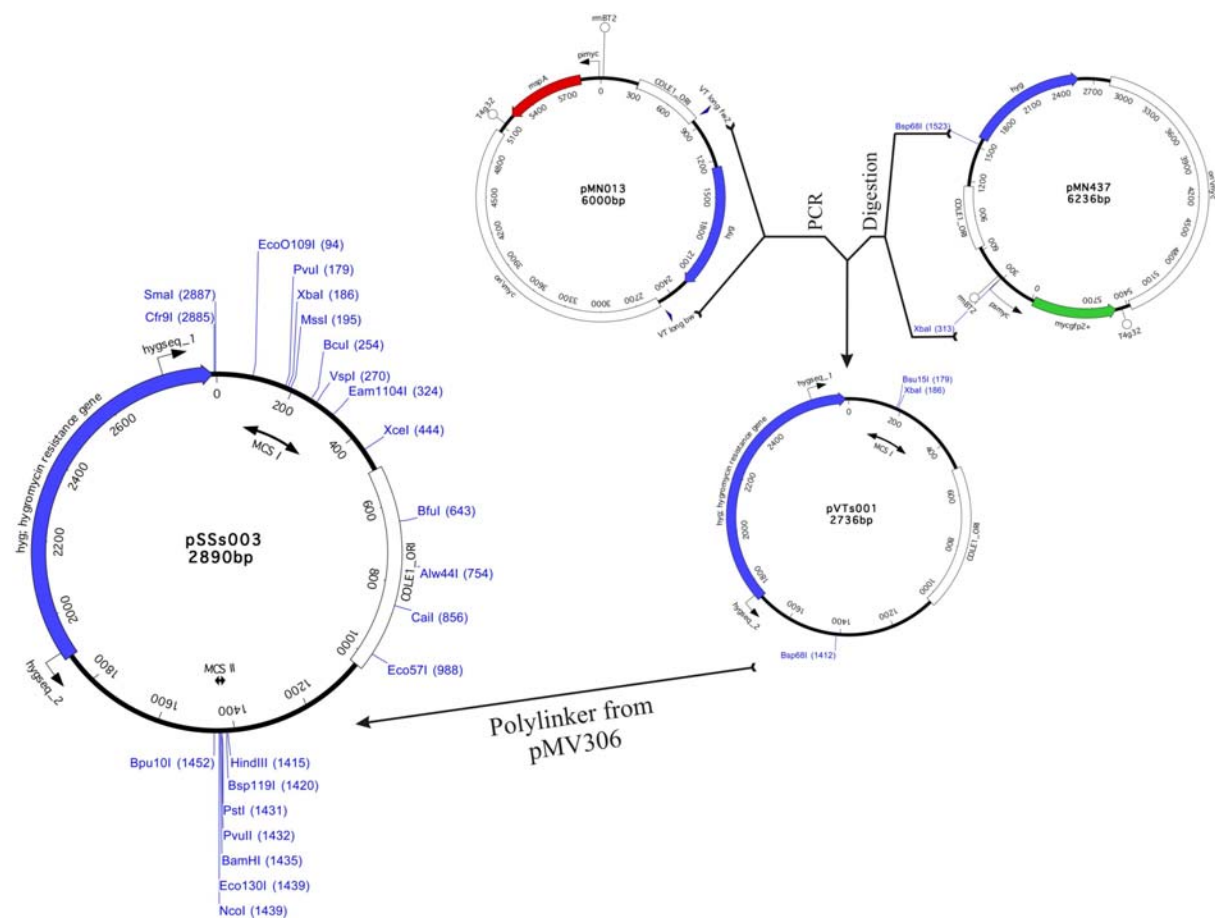


**Figure 19:** Construction and map of the suicide plasmid pSSs003. It possesses two multiple cloning sites (MCS), which flank the hygromycin resistance gene *hyg*. The binding sites for sequencing primers to prove the inserted sequences are indicated as *hygseq\_1* and 2.

Currently the flanking regions of *porM1* from *M. fortuitum* 10851/03 are transferred into both multiple cloning sites (Figure 20) and mutagenesis experiments have started. Deletion of *porM1* in *M. fortuitum* will provide an option to analyze the role of porins on pathogenicity of the species. This plasmid is also currently employed to delete the genes for the DNA binding proteins *mdp1* in *M. bovis* BCG and *hlp1* in *M. smegmatis* (data not shown).

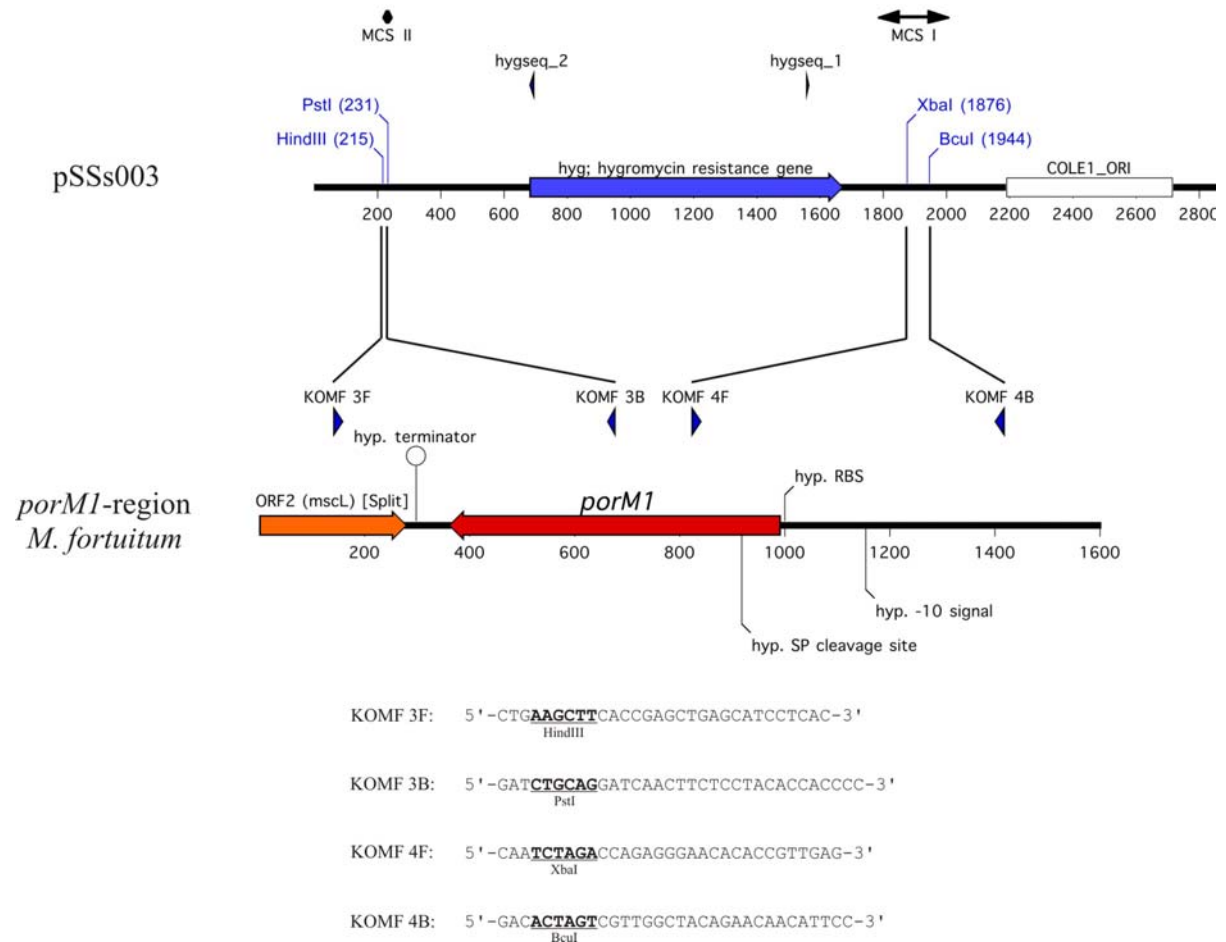


**Figure 20:** Cloning of flanking regions of *porM1* in pSSs003. Parts of *porM1* and its flanking regions were obtained by means of PCR using the primer pairs KOMF 3F/3B and KOMF 4F/4B. These primers introduce the restriction sites as indicated by the underlined and bold letters, which enable the cloning of the PCR fragments in the relative restriction sites of pSSs003.